AGU PUBLICATIONS

JGR

Journal of Geophysical Research: Atmospheres

RESEARCH ARTICLE
10.1002/2017JD026820

A Methodology to Adjust ATMS Observations for Limb Effect and Its Applications

Kexin Zhang[1], Lihang Zhou[2], Mitch Goldberg[3], Xingpin Liu[1], Walter Wolf[2], Changyi Tan[1], and Quanhua Liu[2]

[1]I.M. Systems Group Inc., Rockville, MD, USA, [2]NOAA/NESDIS/STAR, College Park, MD, USA, [3]NOAA JPSS office, Lanham, MD, USA

Key Points:
- The undesirable feature of cross-track sounders is that the measurements vary with scan angle due to limb effect
- Our limb correction approach is to limb adjust the measurements to a fixed view angle
- The limb corrected brightness temperature imagery presents snapshots for quick weather signal diagnosis, such as warm cores in tropical cyclones

Correspondence to:
K. Zhang,
kexin.zhang@noaa.gov

Citation:
Zhang, K., Zhou, L., Goldberg, M., Liu, X., Wolf, W., Tan, C., & Liu, Q. (2017). A methodology to adjust ATMS observations for limb effect and its applications. *Journal of Geophysical Research: Atmospheres*, *122*, 11,347–11,356. https://doi.org/10.1002/2017JD026820

Received 21 MAR 2017
Accepted 3 OCT 2017
Accepted article online 25 OCT 2017
Published online 3 NOV 2017

Abstract The Advanced Technology Microwave Sounders (ATMS), carried on the Suomi National Polar-orbiting Partnership (SNPP) satellite, was launched on 28 October 2011. The ATMS is a follow-on instrument to advanced microwave sounding unit (AMSU), currently flying on National Oceanic and Atmospheric Administration (NOAA) satellites. The primary new ATMS features are a reduced hardware package and improved gap coverage. One thing in common about cross-track sounders is a scan perpendicular to the motion of the satellite, allowing a broad swath of measurements to be taken. But an undesirable feature is that the measurements vary with scan angle because of changes in the optical pathlength through the Earth's atmosphere between the Earth and the satellite. One approach to this problem is to limb adjust the measurements to a fixed view angle. The limb correction algorithm applied to ATMS is based on the heritage methodology originally applied to MSU and later to AMSU. The limb correction method is applied to each of the 96 ATMS field of view (FOV) per scan line, adjusting the off-nadir FOV to the nadir view with fitting error generally within the instrumental noise. The limb-adjusted brightness temperature were used in the original, legacy TIROS Operational Vertical Sounder, and Advanced TIROS Operational Vertical Sounder NOAA sounding product algorithms and more recently to derive the total precipitation water (TPW) retrieval over ocean, with a bias of 0.046 mm and a standard deviation of 3.43 mm, when compared with European Centre for Medium-Range Weather Forecasts TPW data. The limb-corrected brightness temperature can be used to detect the atmospheric weather features, such as the warm cores for tropical cyclones, and the imagery presents snapshots for quick weather signal diagnosis.

1. Introduction

The Advanced Technology Microwave Sounders (ATMS) is a microwave radiometer carried onboard the Suomi National Polar-orbiting Partnership (SNPP) satellite launched in October 2011. SNPP is the first satellite designed to bridge into the next generation National Oceanic and Atmospheric Administration (NOAA) Joint Polar Satellite System (JPSS) satellite constellation. The ATMS combines the capabilities of current generation microwave temperature sounders (Advanced Microwave Sounding Unit-A, AMSU-A) and microwave humidity sounders (Advanced Microwave Sounding Unit-B, AMSU-B) that are flying on NOAAs Polar-orbiting Operational Environmental Satellites (POES), with higher spatial resolution and better calibration accuracy (Weng & Yang, 2016). The ATMS radiances are assimilated into numerical weather prediction (NWP) models worldwide and have been shown to provide impact on global and medium range NWP (Goldberg et al., 2013; Zhou et al., 2016). The ATMS operates in conjunction with the Cross-track Infrared Sounder (CrIS), to provide atmospheric sounding information. The NOAA Unique Combined Atmospheric Processing System products from SNPP are currently ingested into the Advanced Weather Interactive Processing System (AWIPS II (AWIPS II Forecasting Software. Available online http://www.unidata.ucar.edu/software/awips2)) for use at Weather Forecasting Offices (WFOs) nationwide for analyzing atmospheric instabilities, potential outbreaks of severe weather, and now-casting applications (Line & Calhoun, 2015).

The ATMS has 22 microwave channels and the frequency dependence of atmospheric absorption allows different altitudes to be sensed by spacing channels along different absorption lines. Individual ATMS channels are carefully chosen based on principles of radiative transfer theory. ATMS channels 1 and 2 provide water vapor, cloud water, and surface emissivity information needed for temperature profile retrieval. Channels 3 through 15, are nearly identical to those of the AMSU-A; only channel 4 is a new addition. Channels 3 through

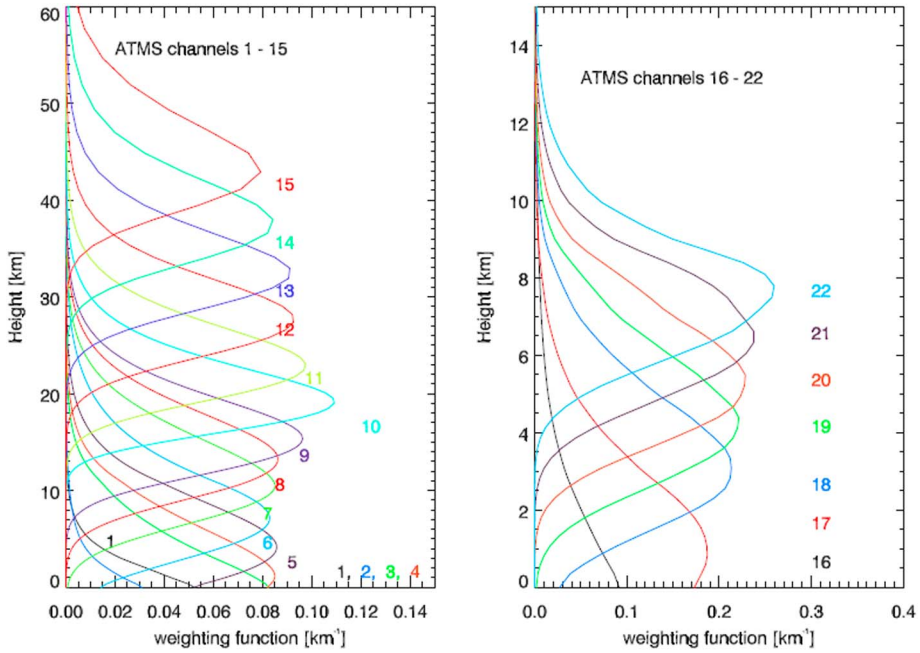

Figure 1. ATMS weighting function of U.S. standard atmosphere over water surface using Community Radiative Transfer Model (CRTM).

15 are the center frequencies of the temperature sounding channels, and most channels are located on both sides of the 57.29 GHz oxygen band to provide temperature soundings to 3 mb (37 km altitude). Channels 18 to 22 are the humidity-sounding group, similar to those on AMSU-B, with two new additions of channels 18 and 19 to further improve the moisture sounding. ATMS has 96 fields of view sampled per scan in a stepped-scan fashion, each separated by 1.11°. The angular range of an ATMS scan is ±52.725° relative to the nadir. The angle-dependent measurements could cause the differences to nadir as large as 30 K at the extreme scan positions in the window channels. An algorithm is needed to calculate limb adjustment coefficients to transform all ATMS data to the values they would have in a nadir view. NOAA has a long history of limb adjustment measurements to fixed view angle to derive the legacy TOVS and ATOVS sounding products (Reale et al., 1994, 2002). The limb adjustment algorithm was originally developed for TOVS (Wark, 1993) and then expanded to ATOVS and AMSU-A data (NOAA 15, 16, 18, and 19) (Goldberg et al., 2001; Liu & Weng, 2007).

This work further expands the legacy limb adjustment coefficients to each of the 22 ATMS channels at each of the off-nadir beam positions. Two sets of coefficients were generated over land and ocean, respectively. Stated simply, the algorithm for adjusting ATMS brightness temperatures to the nadir is a linear combination of two or three closely (physically and statistically) associated channels. One of the advantages of limb-corrected observations is to simplify the regression retrieval process by eliminating the need for scan-dependent sampling of observations for product tuning (Reale et al., 2002). The limb-corrected AMSU-A brightness temperatures have been used in temperature retrievals (Goldberg, 1999; Reale et al., 2002). This paper describes and assesses the limb correction method applying it to ATMS measurement, and it also introduces its application in total precipitable water retrievals over the ocean and tropical cyclone warm core detection.

2. The Procedure of Limb Correction

2.1. The Limb Adjustment Algorithm

This method assumes that the limb effect can be compensated for using linear combinations of the channels at a given angle (Wark, 1993) as expanded for AMSU in Goldberg et al. (2001) paper. The predictors used in the training ensemble are mean brightness temperatures within 2° latitude bands of the chosen channels at each beam position. The number of predictors is generally decided by the channel itself (predictand) plus the adjacent channels whose weighting functions peak directly below and above, which also have strong statistical correlations with the channel of interest. The selection of associated channels will be discussed in the next section. Figure 1 shows the weighting function using Community Radiative Transfer Model (CRTM) (Liu & Boukabara, 2014; Weng et al. 2005) to compute the weighting function at nadir for U.S. standard

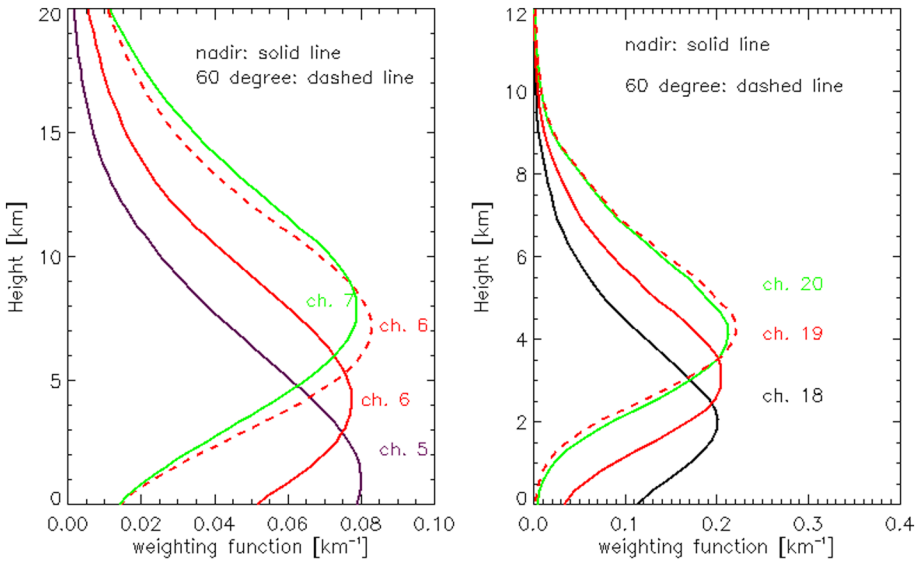

Figure 2. ATMS channels 6 and 19 weighting functions of U.S. standard atmosphere over water surface using Community Radiative Transfer Model (CRTM) shift up in altitude from nadir (solid curve) to 60° (dashed); ATMS channel 5, 7, 18, and 20 were plotted as references.

Table 1
Selection of Associated Channels as Predictors for Each ATMS Channel

Frequency (GHz)	ATMS channel	Associated channels	Peak WF (hPa)
23.8	1	1, 2	Surface
31.4	2	1, 2	Surface
50.3	3	3, 4, 5	Surface
51.76	4	3, 4, 5	Surface
52.8	5	4, 5, 6	1,000
53.596 ± 0.115	6	5, 6, 7	700
54.4	7	6, 7, 8	400
54.94	8	7, 8	270
55.5	9	9, 10, 11	180
$f_0 = 57.29$	10	10, 11	90
$f_0 \pm 0.3222 \pm 0.217$	11	10, 11, 12	50
$f_0 \pm 0.3222 \pm 0.048$	12	11, 12, 13	25
$f_0 \pm 0.3222 \pm 0.022$	13	12, 13	12
$f_0 \pm 0.3222 \pm 0.010$	14	12, 13, 14	5
$f_0 \pm 0.3222 \pm 0.0045$	15	14, 15	2
88.2	16	1, 16	surface
165.5	17	17, 18	1,000
183.31 ± 7	18	18, 19	800
183.31 ± 4.5	19	18, 19, 20	700
183.31 ± 3	20	19, 20, 21	600
183.31 ± 1.8	21	20, 21, 22	500
183.31 ± 1	22	21, 22	450

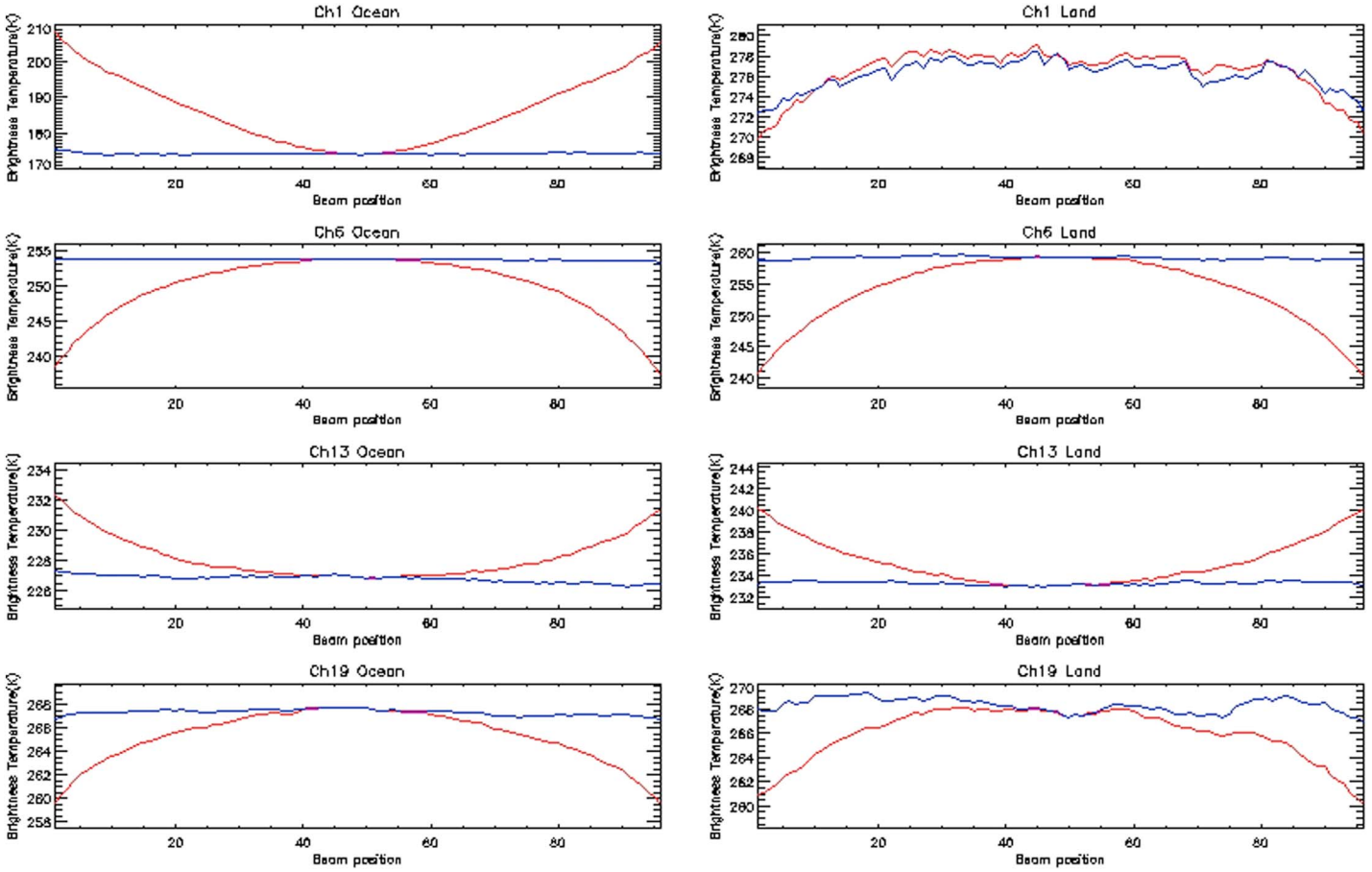

Figure 3. Mean unadjusted versus limb-corrected brightness temperatures (with latitude between ±60°) as a function of beam position over (left column) ocean and (right column) land on 9 June 2015 for ATMS channels 1, 6, 13, and 19. (Red line represents unadjusted, and blue line represents adjusted.)

atmosphere over a water surface. ATMS channels 1–4 (23–51.76 GHz), channel 16 (88.2 GHz), and channel 17 (165.5 GHz) are window channels; the contributions from the atmosphere increase the brightness temperature with increasing optical depth; ATMS channels 5–9 (52.8–55.5 GHz) have the peaks of their weighting functions in the troposphere, where the temperature profiles decrease with height; ATMS channels 10–15 (57.29 GHz) have the peaks of weighting functions in the stratosphere, the temperature profiles increase with height; ATMS channels 18–22 (183 GHz) are water vapor channels, which are sensitive to upper and lower tropospheric humidity. The increase in the optical path as the instrument scans from near nadir to extreme beam positions causes the peak of the channel weighting functions to shift up in altitude. Figure 2 illustrates the shift of weighting functions of ATMS channels 6 and 19 from their nadir angle to the extreme angle of 60°. The channel itself and the adjacent channels whose weighting functions peak below and above are selected associated channels as predictors in most channels. For example, for channel 6, the predictor channels are channels 5, 6, and 7 and for channel 19, they are channels 18, 19, and 20. Table 1 lists the predictors we used for each channel, which always include the predictand channel itself. It is critical to update the limb correction coefficient periodically, such as annually, because the training data sets needs to expand to cover the maximum possible range. Furthermore, if one associated channel stops working, we need to adjust the candidate associated channels and train the limb correction coefficients from different but eligible predictor channels.

The limb-corrected brightness temperature is estimated by

$$\widehat{\overline{Tb(i,j)}_n} = \overline{Tb(i)} + \sum_{j^a} a_{i^a j}(i)\left(Tb(i^a,j) - \overline{Tb(i^a,j)}\right) \quad (1)$$

where $\widehat{\overline{Tb(i,j)}_n}$ is the estimated nadir brightness temperature at a certain channel i for beam position j and n represents nadir. In training, we use the average of mean brightness temperature of position 48 and 49 at a certain channel i as the predictand. $\overline{Tb(i)}$ is the expected value of brightness temperature at channel i,

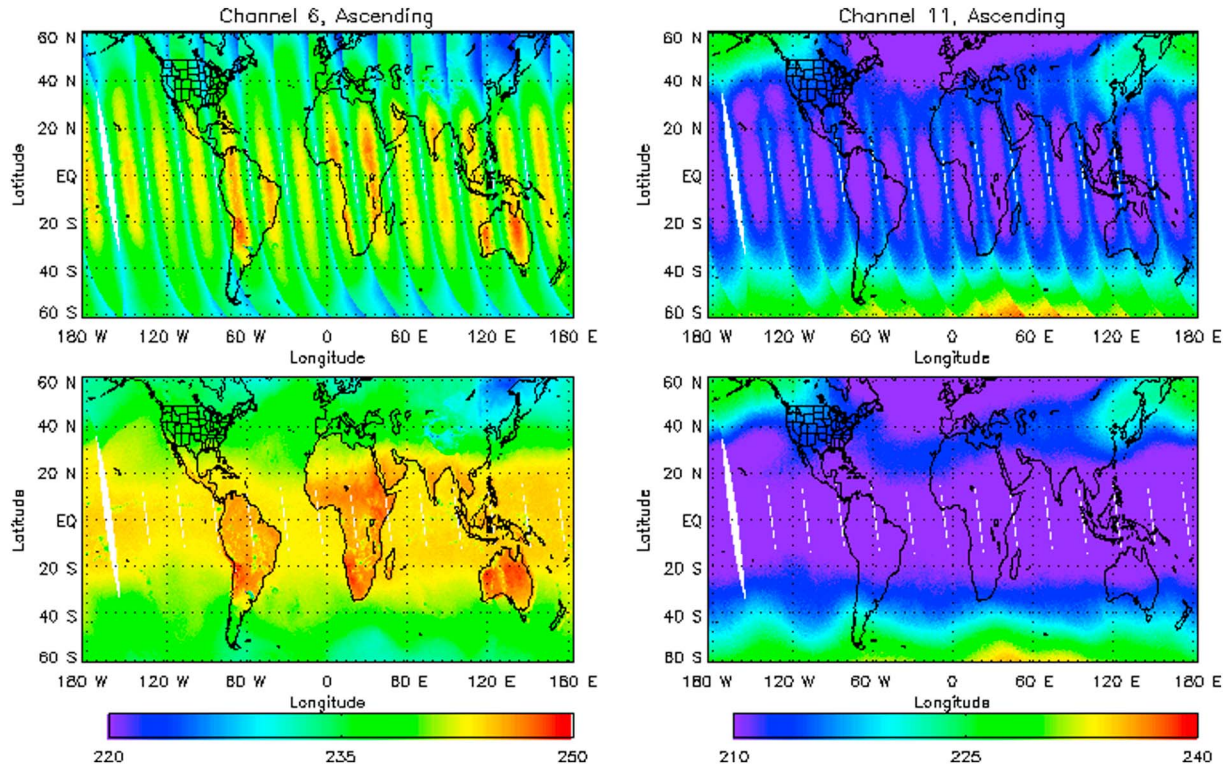

Figure 4. ATMS brightness temperature global map for channels 6 and 11 ascending orbits on 20 December 2014 before and after limb adjustment.

which is the mean of the training sample and was saved in the coefficient file, as is $\overline{Tb(i^a,j)}$. $Tb(i^a,j)$ and $\overline{Tb(i^a,j)}$ are the individual and mean brightness temperatures of "associated" channels i at beam position j, respectively; $a_{i^a j}(i)$ are the regression coefficients calculated by least squares technique from a large ensemble of brightness temperatures. It has been assumed (Wark, 1993) that if a very large sample is used, the mean values in a narrow latitude band, such as 2° in this study, at each beam position will represent the angular variation of a mean meteorological condition of atmospheric parameters. The tests of validity of the procedure that the latitudinal means represent the individual sets of measurments have been discussed in the paper of Wark (1993). We used ATMS Temperature Data Record (TDR) and Geolocation (GEO) data with 22 channels at their original field of view resolution, 96 field of views (FOVs) of brightness temperatures to calculate limb correction coefficients. Two months data of January and September 2014 were used to compute mean brightness temperatures within 2° latitude bands for each FOV. The smoothed latitudinal means represent individual sets of observations over a broad range of meteorological conditions and therefore satisfy the angular brightness temperature requirements placed on the algorithm. A land/sea split in the data was deemed desirable for the surface and near surface channels for the calculation of limb adjustment coefficients because of the difference in emissivity between land and sea. Separate sea and nonsea coefficients are used for channels affected by surface—ATMS channels 1–6 and 16–22. ATMS channels 7–15 use all of the available data to compute coefficients. These sets of coefficients are then merged into two sets: one for land and the other for sea. The natural separation of atmospheric types and cloudiness by latitude and surface types assures that a wide variety is encompassed and that the use of these means in the limb adjustment algorithm is valid. Over ocean, the emissivity at the microwave frequencies is quite low, which results in very low brightness temperatures. Over land, the emissivity is closer to unity, limiting the contrast with the atmospheric contribution, which makes the limb correcting over land more difficult.

Figure 3 demonstrates the average amount of the unadjusted (red line) versus limb-corrected (blue line) ATMS brightness temperature as a function of 96 beam positions. We used 1 day (9 June 2015) data and showed the comparison results over land and ocean. ATMS channels 1–4 are window channels. Statistically, the angular distributions show limb brightening over the ocean due to the low ocean surface emissivity, while atmosphere appears relatively warm. The angular distributions show limb darkening over the land due to the high land surface emissivity, while the atmosphere appears relatively cold. Channel 5–9 sense

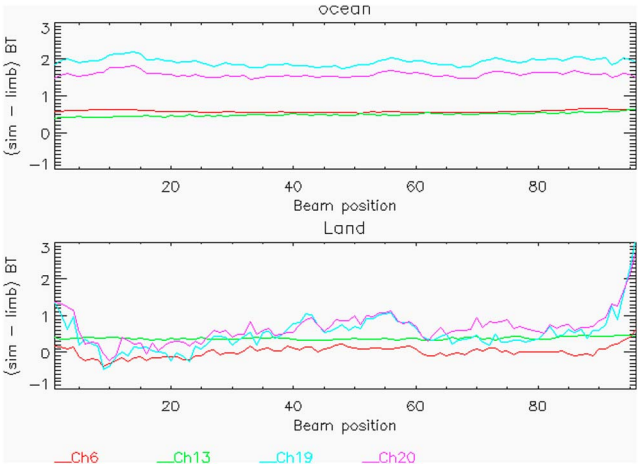

Figure 5. Mean bias between simulated and limb-adjusted ATMS adjusted brightness temperature of 20 December 2015 over (top) ocean and (bottom) land for ATMS channels 6, 13, 19, and 20.

temperatures in the troposphere, and their angular distributions show limb darkening. Channels 10–16 sense temperature in the stratosphere, and their angular distributions show limb brightening. Channels 18-22 sense tropospheric humidity, and their angular distributions show limb darkening. We picked channels 1, 6, 13, and 19 to represent these limb effects and show the limb-corrected brightness temperature. It shows that the limb adjustment effectively removes the scan angle dependence of observed brightness temperature and keep the variation of the signatures from scenes. The limb correction over land has the similar performance as over ocean in atmospheric and water vapor channels, but a little worse in window channels because the land surface emissivity varies in time and space with surface types, roughness, and moisture content.

Figure 4 shows a global image of ATMS channels 6 and 11 observations before and after limb adjustment on 20 December 2014. Due to the polar orbit overlap, we just showed the global map with latitude within 60°. ATMS channel 6 is representative of a lower tropospheric channel with peak sensitivity in the vicinity of 700 mb. We can see the limb darkening at the extreme scan positions, which results in the different brightness temperatures even in an otherwise horizontally homogeneous atmosphere having a homogeneous surface as a background. The limb-adjusted brightness temperature global distribution shows more detailed meteorological structures. Due to the large surface emission over land, this channel still shows the brightness temperature contrast between land and ocean. For channels peaking well above the surface, the land versus sea differences due to emissivity are not evident, such as channel 11. Channel 11 senses temperatures at level above the tropopause and shows limb brightening at the extreme scan positions.

2.2. Selection of Associated Channels

ATMS has 22 channels which provides a broad range of channels for limb adjustment. The selection of associated channels in our study was performed by computing all possible combinations of channels with two or three associated channels. The difficulty is that we do not have true nadir observation at each beam position to compare with, and the angular variation is hard to quantify. Simulated brightness temperature of nadir view for each FOV is a good substitute truth that we rely on. In our study, the simulated ATMS brightness temperature at nadir view is calculated using microwave forward model (Rosenkranz & Barnet, 2006) for one day (20 December 2015), with profiles from collocated European Center for Medium-Range Weather Forecasts (ECMWF). We used the comparison of simulated nadir values with the limb-corrected brightness temperature measurements to select channels. The causes of the systematic errors and uncertainties in observations and simulations using radiative transfer models at 183 GHz have been reviewed by Brogniez et al. (2016). Therefore, the discussion of the systematic differences between limb-corrected measurements and simulated nadir values, although interesting, is outside the scope of this study. We rather focused on getting the optimal associated channel combination in order to achieve least view angle-dependent bias. After a careful scrutiny of the results, the associated channels were selected as shown in Table 1. The comparison with simulated nadir values shows less angle dependence and gives confidence in the overall performance of the limb correction coefficients.

3. Validation and Application

3.1. Validation

Figure 5 shows bias across the scan for limb-corrected-minus-simulated "nadir" values from RTA, over ocean and land for atmospheric and water vapor sounding channels 6, 13, 19, and 20. The simulation of window channels is more difficult due to the surface inhomogeneity, such as the influences of surface emissivity, surface roughness, cloud liquid water, and water vapor. In the atmospheric sounding channels, the limb adjusted and simulated brightness temperatures show good agreement. The systematic differences in water vapor channels could result from radiative transfer modeling errors, ECMWF forecast systematic errors, and limb correction model errors. This figure shows the mean bias of global brightness temperature distribution between limb adjusted and calculated, which indicates little view angle dependence. More accurate surface emissivity model used in the RTA model could be helpful. The mean square error of fit using the associated channels in Table 1 varies with beam positions, and it decreases markedly as the nadir is approached. It is more valuable

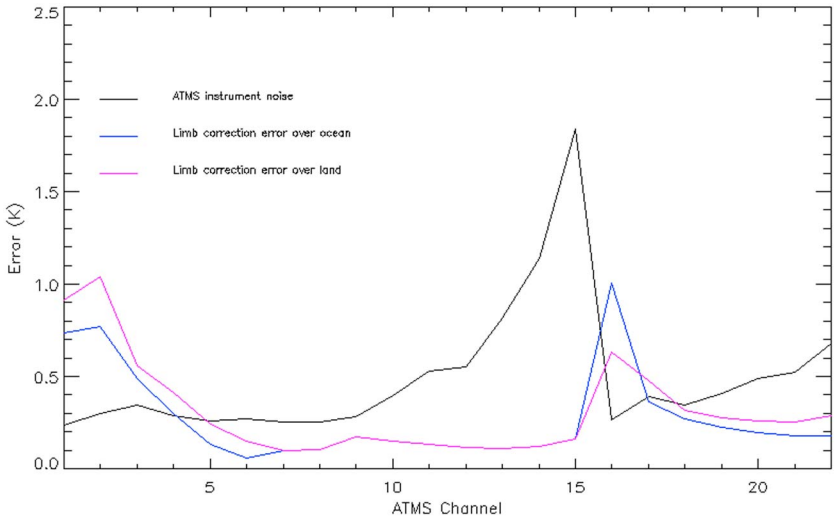

Figure 6. The ATMS limb correction model error versus ATMS on-orbit instrumental noise for each channel.

to look at the mean values to get proper insight into the magnitude of errors arising from the application of the limb adjustment method. Figure 6 illustrates this mean value for each ATMS channel compared with ATMS on-orbit instrument noise. One criteria of channel selections as associated channels is the minimization of noise amplification. The estimated errors of fit should be less than the noise of the instrument. For the atmospheric channels, the land and ocean limb correction coefficients are the same, because they are less affected by the surface. The model errors, both over land and ocean, in most channels are within instrumental noise, except window channels due to surface and cloud liquid water contamination.

3.2. Application

3.2.1. TPW Retrieval Over Oceans

The advantage of retrievals of TPW over ocean is that the lower emissivity of the ocean surface offers a stronger signal for TPW due to the higher atmospheric and surface contrast, and it is very useful for many applications. It has been used in the prediction of the precipitation and for the study of the water cycle in general. Grody et al. (2001) and Weng et al. (2003) used AMSU window channel measurement to derive TPW and the optimal channel combination was the linear combination of 23.8 and 31.4 GHz. In our study, the limb-corrected ATMS brightness temperature of channels 1 (23.8 GHz) and 2 (31.4 GHz) are used as predictors to retrieve total precipitable water (TPW) over ocean. At ATMS lower frequencies, the scattering from cloud liquid is neglected, and the TPW retrieval is linearly derived from these two channels. The coefficients are derived using least squares regression algorithm.

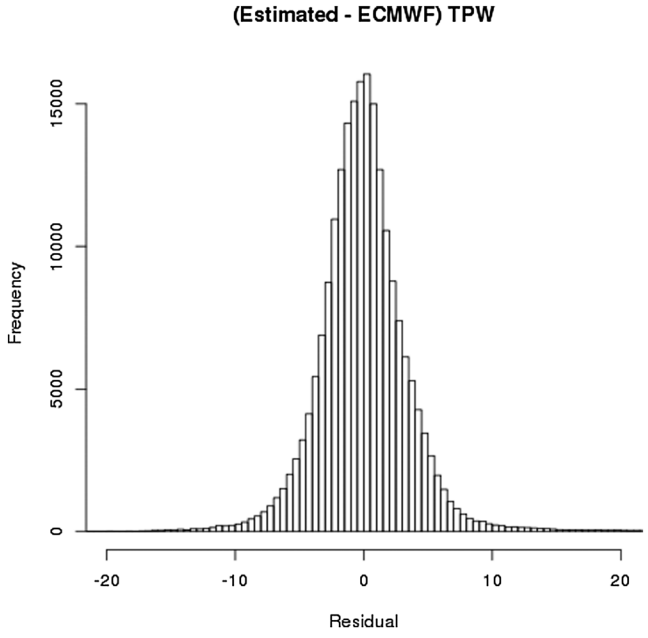

Figure 7. Histogram of Estimated TPW versus ECMWF TPW of 20 December 2014, mean = −0.046 mm and SD = 3.43 mm.

The regression formula is expressed similarly to equation (5a) used in Grody et al. (2001), but the coefficients are not angle dependent.

$$\widehat{\mathrm{TPW}} = a_0 - a_1 \times \ln(285 - bl1) + a_2 \times \ln(285 - bl2), \quad (2)$$

where $bl1$ and $bl2$ are limb-corrected ATMS brightness temperature in channels 1 and 2. The regression coefficient a_0, a_1, and a_2 are trained against ECMWF TPW data (the vertical integration of the atmospheric moisture profile) on 17 February 2015, and $a_0 = 85.67583$, $a_1 = -109.0937$, and $a_2 = 93.71552$. We only perform retrievals for the cases whose limb-corrected brightness temperature are less than 285 K. The latitudes are restricted between 50°S and 50°N to avoid ice surface. If the retrieved TPW is larger than 80 mm, we force it to equal 80 mm. The independent data set on 20 December 2014 has been used as the testing of TPW retrieval algorithm. Figure 7 shows the histogram of residual between estimated and ECMWF TPW, and the bias is −0.046 mm and standard deviation is 3.43 mm.

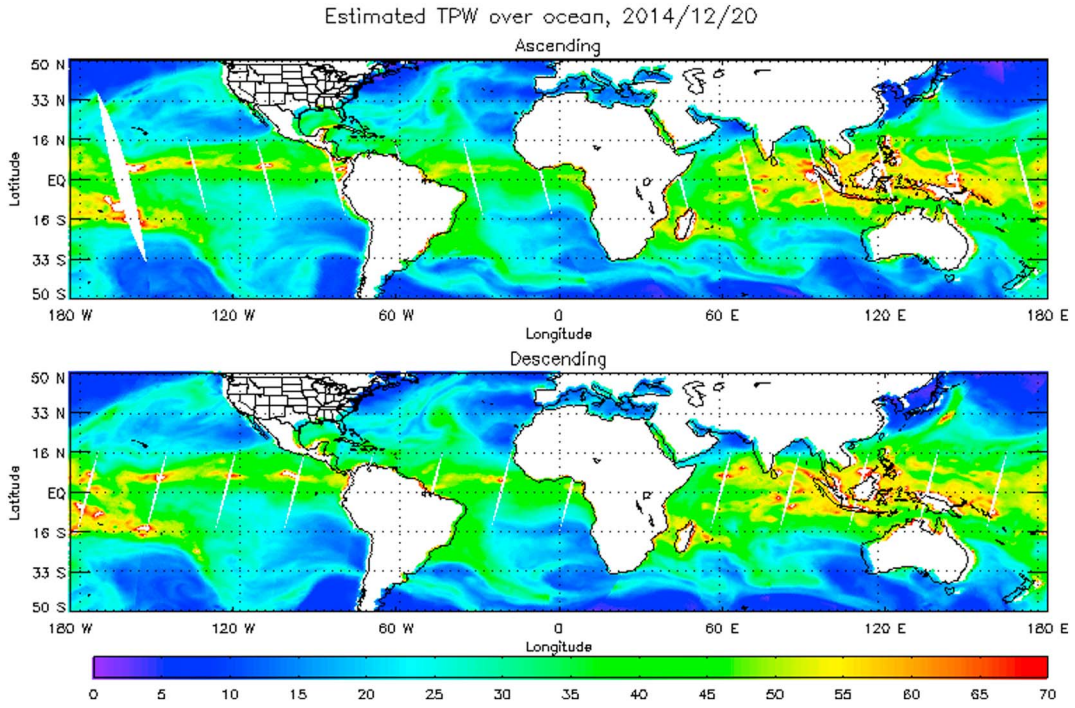

Figure 8. Global distribution of total precipitable water estimated from limb-corrected ATMS over ocean on 20 December 2014.

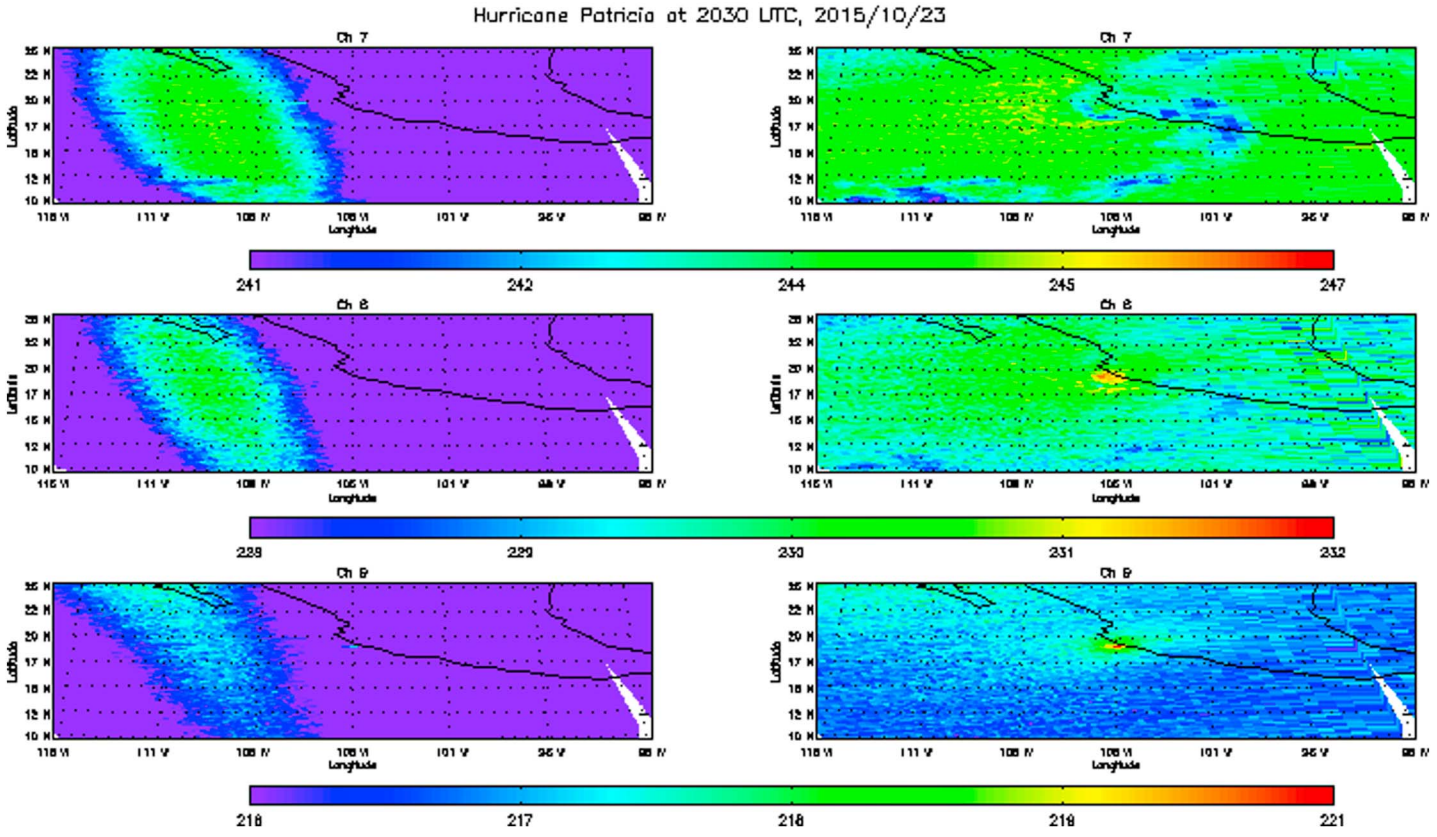

Figure 9. Comparison of ATMS brightness temperature in channels 7, 8, and 9 before and after limb correction over Hurricane Patricia at 2030 UTC 23 October 2015. (top row) Channel 7, (middle row) channel 8, and (bottom row) channel 9; (left column) before and (right column) after.

Figure 8 shows the global distribution of estimated TPW over ocean for both ascending and descending orbits. The TPW global map derived from the limb-adjusted ATMS brightness temperature can be generated in a near real-time manner and compares well with ECMWF TPW. It provides a snapshot for a quick and qualitative look, allowing forecasters to catch up TPW features.

3.3. Tropical Cyclone Monitoring

Because several frequencies in the microwave spectrum are transparent to cirrus clouds, the microwave imagery can reveal some features beneath extensive cover. As tropical storms develop into hurricanes, they are characterized by upper tropospheric warming as a result of adiabatic warming/compression of air as it sinks within the storm center. Subsidence within a tropical cyclone warms the overlying troposphere, suppressing clouds, and leads to the characteristic "eye" commonly observed in satellite pictures. Channels 7–9 are temperature sounding channels located at different elevations within the troposphere and measure the storm related warming. The case we studied is Hurricane Patricia, and the Suomi NPP satellite passed over it on 23 October 2015, 2030 UTC. The eye of Hurricane Patricia was located near 17.3N–105.6W at 1200 UTC. Figure 9 shows that the limb-corrected brightness temperature successfully detected the warm core of the hurricane in channels 7–9 compared with the measured ATMS TDR data at 2030 UTC. Channel 7 (54.4 GHz) peaks near 400 mb, having a weak warm anomaly at the center of the storm. Surrounding this warm anomaly are bands of colder anomalies produced by the effect of scattering due to the strong convection that contain significant concentrations of ice. Channel 8 (54.94 GHz) and channel 9 (55.5 GHz) peak higher into the atmosphere where are not affected by precipitation, and the warm anomalies associated with Patricia are more apparent.

4. Summary

A methodology and application of limb-corrected ATMS brightness temperatures has been presented. The approach is to adjust the off-nadir observation to the average of the two nearest nadir positions using a linear regression based on two or three associated ATMS channels. Limb adjustment model fitting errors are generally within instrumental noise, except for the window channels, where surface inhomogeneity limits the validation. We used the comparison between simulated brightness temperature at nadir and limb-corrected values to select associated channels in order to determine optimal sets per channel. Such differences are also used to validate the limb correction data using independent data over both land and ocean. The results show minimal view angle dependence. Users can use the limb-corrected ATMS imagery for various applications such as TPW retrieval and weather pattern diagnose. For example, the limb-adjusted temperature has been used to retrieve TPW over ocean with bias and standard deviation of −0.046 mm and 3.43 mm, respectively, and to verify tropical cyclone warm cores as snapshots for users to quickly diagnose weather signals.

Acknowledgments

This study is funded by the NOAA JPSS Program Office. The manuscript contents are solely the opinions of the authors and do not constitute a statement of policy, decision, or position on behalf of NOAA or the U.S. Government. The authors also thank the NOAA's Comprehensive Large Array Data Stewardship System (CLASS) to provide ATMS TDR/GEO data. The limb-corrected ATMS granule data files can be accessed via https://www.star.nesdis.noaa.gov/data/publications/ZhangK/ZhangK_JGR-Atmospheres_201709Data.tar.

References

Brogniez, H., English, S., Mahfouf, J.-F., Behrendt, A., Berg, W., Boukabara, S., … Wang, J. (2016). A review of sources of systematic errors and uncertainties in observations and simulations at 183 GHz. *Atmospheric Measurement Techniques*, *9*, 2207–2221. https://doi.org/10.5194/amt-9-2207-2016

Goldberg, M. D. (1999). *Generation of retrieval products from AMSU-A: Methodology and validation*. Paper presented at Tech. Proc. 10th Int. TOVS Study Conference (pp. 215–229). Boulder, CO: Bureau of Meteorological Research Center.

Goldberg, M. D., Crosby, DavidS., & Zhou, Lihang (2001). The limb adjustment of AMSU-A observations: Methodology and validation. *Journal of Applied Meteorology*, *40*, 70–83.

Goldberg, M. D., Kilcoyne, H., Cikanek, H., & Mehta, A. (2013). Joint Polar Satellite System: The United States next generation civilian polar-orbiting environmental satellite system. *Journal of Geophysical Research: Atmospheres*, *118*, 13,463–13,475. https://doi.org/10.1002/2013JD020389

Grody, N., Zhao, J., Ferraro, R., Weng, F., & Boers, R. (2001). Determination of precipitable water and cloud liquid water over oceans from the NOAA 15 advanced microwave sounding unit. *Journal OF Geophysical Research*, *106*(D3), 2943–2953. https://doi.org/10.1029/2000JD900616

Line, W., & Calhoun, K. (2015). *GOES-R and JPSS proving ground demonstration at the 2015 Spring Experiment Experimental Warning Program (EWP) and Experimental Forecast Program (EFP)*. Norman, OK: NOAA Hazardous Weather Testbed (HWT).

Liu, Q., & Boukabara, S. (2014). Community Radiative Transfer Model (CRTM) applications in supporting the Suomi National Polar-orbiting Partnership (SNPP) mission validation and verification. *Remote Sensing of Environment*, *140*, 744–754.

Liu, Q., & Weng, F. (2007). Uses of NOAA-16 and -18 satellite measurements for verifying limb-correction algorithm. *Journal of Applied Meteorology and Climatology*, *46*, 544–548.

Reale, A. L., Chalfant, M. W., Gardner, T. J., & Casey, L. W. (1994). Gardner and TOVS operational sounding upgrades: 1990–1992 (*NOAA Technical Report NESDIS 76*). Washington, DC: US Department of Commerce.

Reale, A. L., Chalfant, M. W., Allegrino, A. S., Tilley, F. H., Ferguson, M. P., & Pettey, M. E. (2002). NOAA operational sounding products for ATOVS (*NOAA Technical Report NESDIS 107*). Washington, DC: US Department of Commerce.

Rosenkranz, P. W., & Barnet, C. D. (2006). Microwave radiative transfer model validation. *Journal of Geophysical Research*, *111*, D09S07. https://doi.org/10.1029/2005JD006008

Wark, D. Q. (1993). Adjustment of TIROS Operational Vertical Sounder data to a vertical view (NOAA Tech. Rep. NESDIS-64) Washington, DC.
Weng, F., & Yang, H. (2016). Validation of ATMS calibration accuracy using Suomi NPP pitch maneuver observations. *Remote Sens*, *8*, 332. https://doi.org/10.3390/rs8040332
Weng, F., Han, Y., van Delst, P., Liu, Q., & Yan, B. (2005). *JCSDA community radiative transfer model (CRTM)*. Paper presented at Tech. Proc. 14th Int. ATOVS Study Conference (pp. 217–222). Beijing, China: World Meteorological Organization.
Weng, F., Zhao, L., Ferraro, R. R., Poe, G., Li, X., & Grody, N. C. (2003). Advanced microwave sounding unit cloud and precipitation algorithms. *Radio Science*, *38*(4), 8068. https://doi.org/10.1029/2002RS002679
Zhou, L., Divakarla, M., & Liu, X. (2016). An overview of the Joint Polar Satellite System (JPSS) science data product calibration and validation. *Remote Sensing*, *8*, 139. https://doi.org/10.3390/rs8020139